Estimating Termination Effect on Electric and Magnetic Field-to-Line Coupling for Radiated Immunity Tests Using a TEM Cell

Chunlei Shi[1, *], Changchun Chai[1], Yintang Yang[1], and Wenxiao Fang[2]

Abstract—An analytic model of the field-to-line coupling in time domain for electrically small lines using a transverse electromagnetic (TEM) cell is proposed in this paper. This model uses mutual capacitance and mutual inductance to represent electric and magnetic field couplings which can be obtained based on voltage and current dividers. The measurement and calculation results validate the accuracy of the model and indicate relevant suppressions for radiated immunity. This model is convenient for fast radiated immunity estimations.

1. INTRODUCTION

Due to the harsh electromagnetic environment, radiated immunity (RI) becomes an essential part of electromagnetic compatibility (EMC) analysis for electronic systems which commonly consist of one or more printed circuit boards (PCBs). Traces on PCBs are one of the key paths to transfer radiated electromagnetic interference (REMI) through EM field coupling into sensitive devices, such as switches, logic circuits and sensors. Therefore, the coupling behavior of PCB traces and EM field is significant for the reliability of electronic systems.

Intensive efforts have been made to find the dependencies of the field-to-line coupling, such as terminal impedance [1–3] and structure [3, 4] of the line. Full-wave electromagnetic solvers are introduced to simulate the behavior of the field-to-line coupling, but this kind of models is complicated for EMC designers to use because of the cumbersome parameters of actual EMI incidence. Recently, transverse electromagnetic (TEM) or gigahertz TEM (GTEM) cell measurements have been widely used for investigations on both line-to-field and field-to-line couplings [3, 5–9], which are specified by international standards [10, 11] for radiated emission and immunity tests, as a low-cost alternative to the measurements over an open-area test site (OATS).

However, previous works investigated field-to-line coupling mostly in frequency domain. In this paper, we propose an analytic model of the field-to-line coupling using TEM cell measurements in time domain. A separation approach has been presented by the authors to quantify the compositions of electric and magnetic field couplings on radiated emissions of a microstrip line with arbitrary terminals [9]. This paper extends the approach to RI tests. Theory verification and measurement results confirm the accuracy of this model.

This paper is organized as follows. The analytic lumped model and theory verification are presented in Section 2. An EMI case application of this model is shown in Section 3. Measurement setup, measured and calculated results are discussed in Section 4. Conclusions are drawn in Section 5.

---

* Corresponding author: Chunlei Shi (shichunlei@xidian.edu.cn).
[1] Xidian University, China. [2] Science and Technology on Reliability Physics and Application of Electronic Component Laboratory, China.

2. AN ANALYTIC LUMPED MODEL OF FIELD-TO-LINE COUPLING

2.1. Circuit Model

A standard TEM cell measurement for RI tests is sketched in Fig. 1. When an EMI signal is injected into a TEM cell, time-varying voltage and current of the EMI generate electric field and magnetic field inside the TEM cell, respectively. The generated electric field induces a common mode current along the microstrip line, whereas the magnetic field induces a differential mode voltage along the line. Since the dimensions of microstrip lines are smaller than $\lambda/10$ at $1\,\text{GHz}$ (the upper frequency of the TEM cell measurement), the phase shift along the lines tends to zero. Consequently, the inductions can be treated as distributed sources along the microstrip line. The induced current source I_{EC} and voltage source V_{MC} of microstrip lines can be written in terms of mutual capacitance C_{TEM} and mutual inductance M_{TEM} [9] and the time-varying EMI signal:

$$I_{\text{EC}} = C_{\text{TEM}}\frac{\partial V_{\text{EMI}}}{\partial t} \tag{1}$$

$$V_{\text{MC}} = M_{\text{TEM}}\frac{\partial I_{\text{EMI}}}{\partial t} \tag{2}$$

where V_{EMI} and I_{EMI} are the time-varying voltage and current of the EMI injected into the TEM cell, respectively.
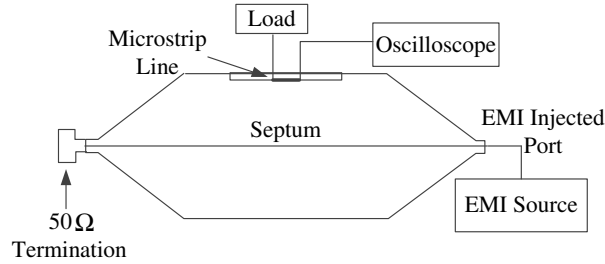
Figure 1. Standard TEM cell measurement for RI test in time domain.

Equivalent models and circuits of electric and magnetic field-to-line couplings between a microstrip line and a TEM cell are shown in Fig. 2. The EMI source is matched to the TEM cell. Thus, the EM field inside the cell can be considered spatially uniform. Since most transmission lines in high-frequency systems have at least one terminal matching, we only investigate the termination effect of one terminal. Therefore, the output impedance Z_{out} is set to match the characteristic impedance of the microstrip line, and the impedance Z_L at the load end of the line is altered.

As the TEM cell approximates a 50-Ω transmission line, electromagnetic waves inside the TEM or GTEM cell propagate along the length direction. Therefore, the microstrip line needs to be placed parallel to the length direction to get electric and magnetic field couplings simultaneously. The induced voltages at both ends of the line by electric field coupling are in phase, while those by magnetic field coupling are out of phase. For RI tests, the maximum magnitude of EMI responses is more relevant. Thus, the output voltage of the microstrip line is located to get the sum of induced voltages:

$$V_{\text{out}} = AI_{\text{EC}}Z_{\text{out}} + BV_{\text{MC}} = AZ_{\text{out}}C_{\text{TEM}}\frac{\partial V_{\text{EMI}}}{\partial t} + BM_{\text{TEM}}\frac{\partial I_{\text{EMI}}}{\partial t} \tag{3}$$

where A and B are the coefficients determined by Z_L at the load end of the line; Z_{out} is the impedance of the oscilloscope at the other end of the line, equal to the characteristic impedance Z_0 of the microstrip line. A and B can be derived from Figs. 2(c) and (d), as voltage and current dividers:

$$A = \frac{Z_L}{Z_L + Z_{\text{out}}} \tag{4}$$

$$B = \frac{Z_{\text{out}}}{Z_L + Z_{\text{out}}} \tag{5}$$
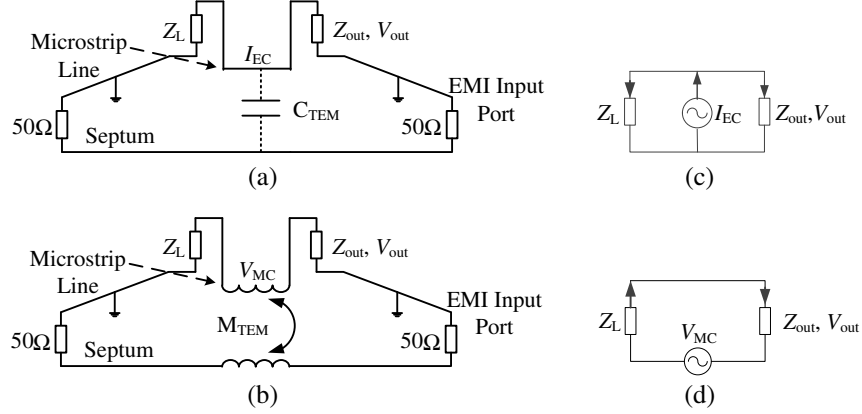
Figure 2. Equivalent models and circuits for electric and magnetic field-to-line couplings between a microstrip line and the septum of a TEM cell: (a) and (c) equivalent models and circuits for electric field-to-line coupling, (b) and (d) equivalent models and circuits for magnetic field-to-line coupling.

2.2. Theory Verification

When the microstrip line is terminated with a load Z_L, the reflection coefficient Γ_0 is commonly used [12] to quantify signal reflection from the load:

$$\Gamma_0 = \frac{Z_L - Z_0}{Z_L + Z_0} \tag{6}$$

Since Z_{out} is matched to Z_0, there is no reflection from the oscilloscope.

Then, the voltage at the output end (the oscilloscope) of the microstrip line is equal to

$$V_{\text{out}} = V^+ + \Gamma_0 V^- e^{-j\beta l} \tag{7}$$

where V^+ is defined as the forward induced voltage wave of the microstrip line to the oscilloscope; V^- is the reflected induced voltage wave from the load. Under excitation of an EMI signal; V^+ and V^- at two ends of the line are both ascribed to electric and magnetic field couplings and expressed as $1/2(V_{\text{EC}} + V_{\text{MC}})$ and $1/2(V_{\text{EC}} - V_{\text{MC}})$, respectively.

Since the line is electrically small, the phase shift βl along the line trends to zero. Then, Eq. (7) can be simplified:

$$V_{\text{out}} = V^+ + \Gamma_0 V^- = \frac{1}{2}(V_{\text{EC}} + V_{\text{MC}}) + \frac{1}{2}\Gamma_0(V_{\text{EC}} - V_{\text{MC}}) = V_{\text{EC}}\frac{Z_L}{Z_L + Z_{\text{out}}} + V_{\text{MC}}\frac{Z_{\text{out}}}{Z_L + Z_{\text{out}}} \tag{8}$$

3. AN EMI CASE

Transmission line pulse (TLP) is a measurement technique widely used in the electrostatic discharge test. In this paper, a TLP signal is used to be the EMI signal. The square shape and accurate fast rise time of TLP TLP can induce a specific response on microstrip lines, which can demonstrate the termination effect on RI clearly. Demonstrations of the voltage shape of the TLP and the response of a shorted 10-mm microstrip line are shown in Fig. 3. It can be seen that the rising and falling edges of the TLP are the effective parts of the EMI signal. Then, the peak response of the microstrip line excited by the rising edge of the TLP can be obtained from Eq. (3):

$$V_p = AZ_{\text{out}}C_{\text{TEM}}\frac{\partial V_{\text{EMI}}}{\partial t}\Big|_{RT} + BM_{\text{TEM}}\frac{\partial I_{\text{EMI}}}{\partial t}\Big|_{RT} \tag{9}$$

In the case of shorted termination ($Z_L = 0$), A is equal to 0 and B equal to 1; in the case of open termination ($Z_L = \infty$) A is 1 and B is 0. When Z_L is matched to the microstrip line, coefficients A

and B are both equal to 0.5. Substituting the values of A and B into Eq. (9), the peak responses of the microstrip line with shorted, open and matched terminations are

$$V_p^S = M_{\text{TEM}}\frac{\partial I_{\text{EMI}}}{\partial t}|_{RT} \tag{10}$$

$$V_p^O = AZ_{\text{out}}C_{\text{TEM}}\frac{\partial V_{\text{EMI}}}{\partial t}|_{RT} \tag{11}$$

$$V_p^M = \frac{1}{2}Z_{\text{out}}C_{\text{TEM}}\frac{\partial V_{\text{EMI}}}{\partial t}|_{RT} + \frac{1}{2}M_{\text{TEM}}\frac{\partial I_{\text{EMI}}}{\partial t}|_{RT} \tag{12}$$

where V_p^S, V_p^O and V_p^M are the peak response voltages of the microstrip line with shorted, open and matched terminations, respectively.
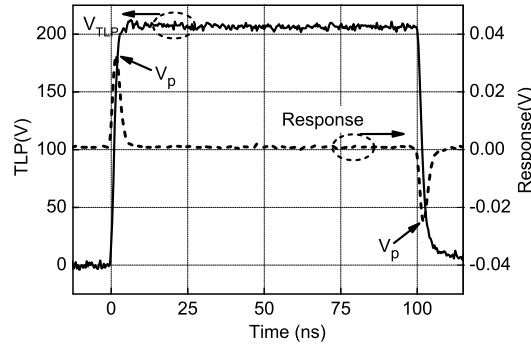
Figure 3. Shape of TLP (solid line) and response (dash line) of microstrip line with shorted termination.

4. MEASUREMENT SETUP AND RESULT DISCUSSION

4.1. Measurement Setup

The scheme of the measurement setup is shown in Fig. 4. The TLP generator is Celestron TLP. The duration of the TLP is 100 ns, and the rise time is 2 ns. The output impedance of the TLP system is $50\,\Omega$, matched to the characteristic impedance of the TEM cell. The TEM cell is FCC-TEM-JM1. The TLP generator was connected to the signal input port of the TEM cell as the EMI source. The other port of the TEM cell was ended with a $50\,\Omega$ load. A microstrip line is fabricated at the center of a square PCB ($= 4.2$) and ended by surface-mount SMA connectors. One end of the microstrip line was connected to an oscilloscope for signal detection and the other end connected to an optional terminal (short, open or $50\,\Omega$). Microstrip lines with two different lengths ($l = 10\,\text{mm}$ and $l = 20\,\text{mm}$) and the same width ($w = 1\,\text{mm}$) were measured. All lines were designed to have a characteristic impedance of $50\,\Omega$.
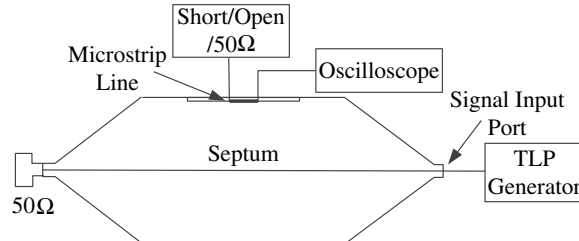
Figure 4. Measurement setup for RI test.
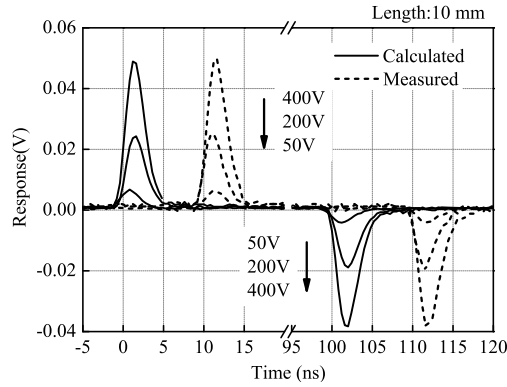
Figure 5. Calculated and measured responses of the 10-mm matched microstrip line excited by 50 V, 200 V and 400 V TLPs.
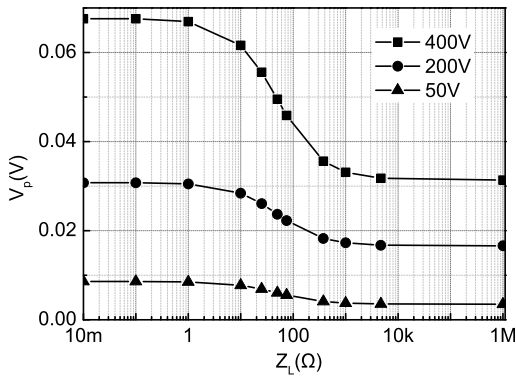
Figure 6. Calculated peak responses V_p of the 10-mm microstrip line with different terminal impedances excited by the rising edge of 50 V, 200 V and 400 V TLPs.
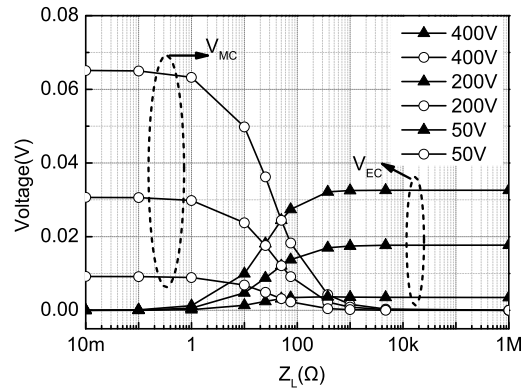
Figure 7. Contribution of electric and magnetic field-to-line couplings on peak response V_p of the 10-mm microstrip line with different terminal impedances excited by the rising edge of 50 V, 200 V and 400 V TLPs.

4.2. Result Discussion

Since the only difference between TLP responses of 10-mm and 20-mm microstrip lines is the amplitude. Hence, the results of the 10-mm line are chosen to illustrate. The calculated and measured TLP responses of the matched microstrip line are plotted in Fig. 5. The agreements of calculation and measurement results validate the accuracy of this analytic model.

The peak response is more relevant to define the lower limitation of the immunity. Therefore, Fig. 6 gives the calculation results of the peak responses V_p of the microstrip line with different terminal impedances, which are excited by the rising edge of different amplitudes of TLPs. The calculation results show that the termination effect on RI is more obvious with the TLP interference enhancing. Under the same TLP incidence, the peak response decreases with increasing terminal impedance of the line.

Figure 7 shows the compositions of electric and magnetic field-to-line couplings on the peak responses V_p in Fig. 6. The results reveal that contributions of electric and magnetic field-to-line couplings to the response are equal for the line matched, $Z_L = 50\,\Omega$; when Z_L is below $50\,\Omega$, most of the peak response is ascribed to the magnetic field coupling; when Z_L is over $50\,\Omega$, most of the peak response is ascribed to the electric field coupling. Thus, for RI predictions, electric field coupling is suppressed when the terminal impedance is below $1\,\Omega$, whereas magnetic field coupling is suppressed when terminal impedance is over $1\,k\Omega$. In real systems, there is a tradeoff between electric and magnetic field couplings to obtain a RI optimization for EMC design.

5. CONCLUSION

In this paper, an analytic circuit model of the time-domain field-to-line coupling is proposed using the TEM cell measurement. The quantities of electric and magnetic field couplings reveal the termination effect on the EMI response and the coupling composition. When the terminal impedance of microstrip lines is higher than the line's characteristic impedance, the EMI response is mainly ascribed to electric field coupling. On the contrary, a microstrip line with the terminal impedance lower than its characteristic impedance responds mainly to magnetic field coupling. This circuit model is simple but helpful for terminal selections and RI predictions in EMC design and analysis.

REFERENCES

1. Lagos, J. L. and F. L. Fiori, "Worst-case induced disturbances in digital and analog interchip interconnects by an external electromagnetic plane wave-Part I: Modeling and algorithm," *IEEE Trans. on Electromagnetic Compatibility*, Vol. 53, No. 1, 178–184, 2011.

2. Magdowski, M. and R. Vick, "Closed-form formulas for the stochastic electromagnetic field coupling to a transmission line with arbitrary loads," *IEEE Trans. on Electromagnetic Compatibility*, Vol. 54, No. 5, 1147–1152, 2012.

3. Land, S. O., M. Ramdani, R. Perdriau, et al., "Using a modified Taylor cell to validate simulation and measurement of field-to-shorted-trace coupling," *IEEE Trans. on Electromagnetic Compatibility*, Vol. 56, No. 4, 864–870, 2014.

4. Land, S. O., T. Mandic, M. Ramdani, et al., "Comparison of field-to-line coupling models: Coupled transmission lines model versus single-cell corrected Taylor model," *Proc. Int. Symp. on Electromagnetic Compatibility (EMC Europe)*, 276–281, 2013.

5. Mandic, T., B. Pejcinovic, and A. Baric, "Comparison of simulation and measurement of time-domain field-to-line coupling in TEM cell," *Proc. Int. Symp. on Electromagnetic Compatibility (EMC Europe)*, 681–685, 2014.

6. Kasturi, V., S. Deng, T. Hubing, et al., "Quantifying electric and magnetic field coupling from integrated circuits with TEM cell measurements," in *Proc. IEEE Int. Symp. Electromagnetic Compatibility*, Vol. 2, 422–425, 2006.

7. Deng, S., T. Hubing, and D. Beetner, "Characterizing the electric field coupling from IC heatsink structures to external cables using TEM cell measurements," *IEEE Trans. on Electromagnetic Compatibility*, Vol. 49, No. 4, 785–791, 2007.

8. Deng, S., T. Hubing, and D. Beetner, "Using TEM cell measurements to estimate the maximum radiation from PCBs with cables due to magnetic field coupling," *IEEE Trans. on Electromagnetic Compatibility*, Vol. 50, No. 2, 419–423, 2008.

9. Shi, C., W. Fang, C. Chai, et al., "Using termination effect to characterize electric and magnetic field coupling between TEM cell and microstrip line," *IEEE Trans. on Electromagnetic Compatibility*, Vol. 57, No. 6, 1338–1344, 2015.

10. "Integrated circuits, measurement of electromagnetic emissions Part 2: Measurement of radiated emissions, TEM cell and wideband TEM cell method," *IEC 61967-2*, 1st Edition, 2005.

11. "Integrated circuits, measurement of electromagnetic immunity Part 2: Measurement of radiated immunity, TEM cell and wideband TEM cell method," *IEC 62132-2*, 1st Edition, 2010.

12. Ludwig, R. and G. Bogdanov, *RF Circuit Design Theory and Applications*, 2nd Edition, Publishing House of Electronics Industry, Beijing, 2010.